

AD-A063 866

BOLT BERANEK AND NEWMAN INC CAMBRIDGE MASS
SOURCE LEVEL MODEL FOR PROPELLER BLADE RATE RADIATION FOR THE W--ETC(U)
JUL 78 L GRAY, D GREELEY

F/G 20/1

UNCLASSIFIED

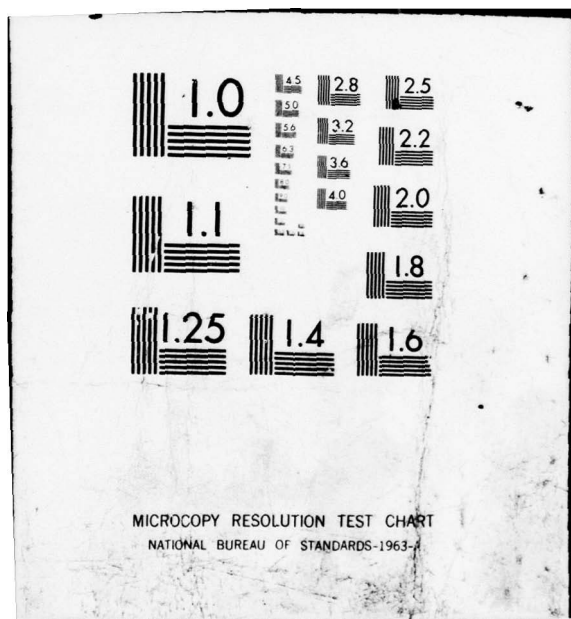
BBN-TM-458

NL

1 OF 1
AD
A063 866



END
DATE
FILED
3-79
DDC



Bolt Beranek and Newman Inc.

BBN

R
sc

Technical Memorandum No. 458

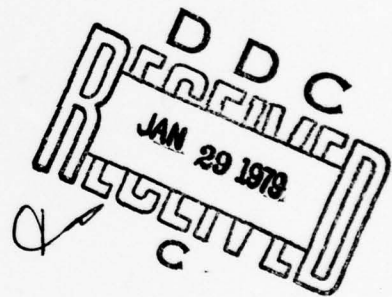
LEVEL

**Source Level Model for Propeller Blade Rate
Radiation for the World's Merchant Fleet**

L. Gray and D. Greeley

DDC FILE COPY

July 1978



Prepared for:
Naval Research Laboratory

This document has been approved
for public release and sale; its
distribution is unlimited.

78 12 11 031

(14)

BBN-TM-458

(1)

TECHNICAL MEMORANDUM NO. 458

(6)

SOURCE LEVEL MODEL FOR PROPELLER BLADE RATE
RADIATION FOR THE WORLD'S MERCHANT FLEET.

(10)

L. J. Gray
D. Greeley

(11)

Jul 19 1978

(9)

Technical
memo



(12)

43 pi

Submitted to:

Naval Research Laboratory
Washington, D.C.
Attention: Mr. Orest Diachok

Submitted by:

Bolt Beranek and Newman Inc.
50 Moulton Street
Cambridge, Mass. 02138

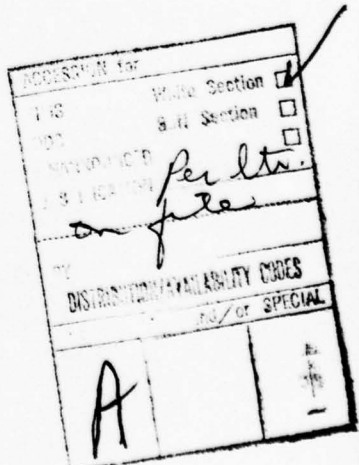
This document has been approved
for public release and codes for
distribution is unclassified

060 100

elt

TABLE OF CONTENTS

	<u>Page</u>
LIST OF FIGURES	
SUMMARY	
1.0 INTRODUCTION	1
2.0 DESCRIPTION OF ACOUSTIC SOURCE	1
2.1 Unsteady Propeller Cavitation-General.....	1
2.2 Propeller Cavitation Time Histories	2
2.3 Radiation from Cavity Volume Changes	10
2.4 Harmonics of Blade Rate	13
3.0 ESTIMATION OF MERCHANT SHIP SOURCE STRENGTHS	13
3.1 Design Limitations for Maximum Unsteady Cavity Volume	13
3.2 Relationship to Obtainable Merchant Ship Parameters	16
3.3 Model for the Dipole Source Strengths of Blade Rate for the World's Merchant Fleet	27
3.4 Model for the Monopole Source Strength and Source Depth of the Merchant Fleet Blade Rate	31
4.0 CONCLUSIONS AND RECOMMENDATIONS	32



LIST OF FIGURES

- Figure 1. Schematic View of Propeller Plane of Single Screw Merchant Vessel.
- Figure 2. Isovelocity Wake Contours for Axial Velocity in Propeller Plane of "Typical" Merchant Vessel.
- Figure 3. Schematic of Propeller Blade Section Inflow Velocity.
- Figure 4. Sheet Cavitation Patterns Observed on Full Size Ship Propellers [3,5].
- Figure 5. Measured Cavity Volume History on Ship Propeller Blade [4].
- Figure 6. Relationship of Higher Harmonics of Blade Rate to First and Second Harmonics [11, 12, 13].
- Figure 7. Total Cavity Volume History on Four Bladed Propeller [4].
- Figure 8. Cavity Volume and Area Relationships for Cambered Marine Propellers.
- Figure 9. Maximum Cavity Volumes Observed on Model and Full Scale Propellers.
- Figure 10. Estimated Propeller Cavity Submergence for Sample Fleet Population.
- Figure 11. Propeller Diameter to Ship Length Relationship for Sample Fleet Population.
- Figure 12. Estimated Distribution of Blade Rate Frequency for the World Fleet of Merchant Vessels.
- Figure 13. Estimated Distribution of Ship Length for the World Fleet of Merchant Vessels (1972).

- Figure 14. Dipole Source Strength at Blade Rate Frequency for the Merchant Fleet Less than 700 Feet in Length.
- Figure 15. Dipole Source Strength at Blade Rate Frequency for the Merchant Fleet over 700 Feet in Length.
- Figure 16. Monopole Source Strength PDF for Blade Rate of the Merchant Fleet less than 700 Feet in Length.
- Figure 17. Monopole Source Strength PDF for Blade Rate of the Merchant Fleet over 700 Feet in Length.

SUMMARY

This memo presents a model for the acoustic source strength of blade rate line energy produced by single screw merchant vessels. These source strengths are based on observed cavitation time histories on merchant vessels, and on limitations imposed by considerations of propeller design procedures and ship vibration criteria. Relationships are presented for the expected value of the blade rate source strength for ships of different lengths, expressed both as a monopole source strength located a known depth below a free surface; and as a dipole source strength which describes the pressure radiated to the far field. These relationships are based on a small sample of merchant ships characteristics and are exercised for the estimated population of ships at sea to yield a statistical description of the distribution of source strength for the world fleet of single screw merchant vessels.

1.0 INTRODUCTION

In order to correctly predict low frequency ocean ambient noise, one must have available a description of the acoustic source levels of merchant ships. The major acoustic source on merchant vessels is propeller cavitation, which characteristically produces both a continuous spectrum component and a set of line components. This line component is generated by the gross changes in the total cavitation volume existing on a ship propeller within one propeller revolution, and consists of a set of harmonically related lines with the fundamental frequency equal to the propeller blade rate.

The purpose of this paper is to present a model for the prediction of the source levels and frequencies of the blade rate acoustic energy generated by propeller cavitation volume changes on merchant ships. This model is exercised for a set of ships representative of the present world merchant fleet, yielding a statistical description of this blade rate line energy for the merchant fleet.

2.0 DESCRIPTION OF ACOUSTIC SOURCE

2.1 Unsteady Propeller Cavitation-General

Marine propellers are designed to produce a given amount of thrust with a given inflow to the propeller. This thrust manifests itself as a pressure reduction on the suction side of the propeller blades. If this pressure reduction on the blades is sufficiently severe, cavitation will occur. The reader is referred to [1] for a discussion of propeller design and the factors influencing propeller cavitation.

On a single screw vessel, there also exists a considerable alternating thrust component due to the fact that the inflow to

to the propeller is considerably non-uniform over the propeller disk. Figure 1 is a schematic of the stern of a vessel showing the ship's propeller and sections of the ship lines perpendicular to the longitudinal ship axis. The inflow to the propeller disk will be affected by the proximity of the hull immediately upstream of the propeller. An example of this inflow (ship wake) for a typical vessel is shown in figure 2, where the contours represent the axial wake velocities normalized on ship speed. Note that there exists a region of low wake velocities near the top of the propeller disk. If a section is taken through the propeller along a radius (figure 3), it is evident that changes in the axial inflow velocity relate directly to changes in the angle of attack on a propeller section. Since the lift on the blade section is proportional to the section angle of attack, and since the amount of cavitation on a section is proportional to both lift and angle of attack, the lift, angle of attack, and total amount of cavitation on a blade will vary as the propeller progresses through the non-uniform wake. The effects of these cavitation volume modulations have been the subject of extensive investigation in recent years due to the importance of cavitation induced pressures in ship vibration excitation. Reference 2, for example, affords a good development of calculation of unsteady propeller cavitation characteristics.

2.2 Propeller Cavitation Time Histories

Histories of propeller cavitation during a revolution as observed on full scale ships have been reported in the literature. References [4,5], for example, measured both cavitation patterns and cavity volumes on an ore carrier propeller using stereo photography. Reference [3] reports observed cavitation patterns on a 250,000 dwt tanker propeller. Both are considered representative of the cavitation existing on merchant ship propellers at full

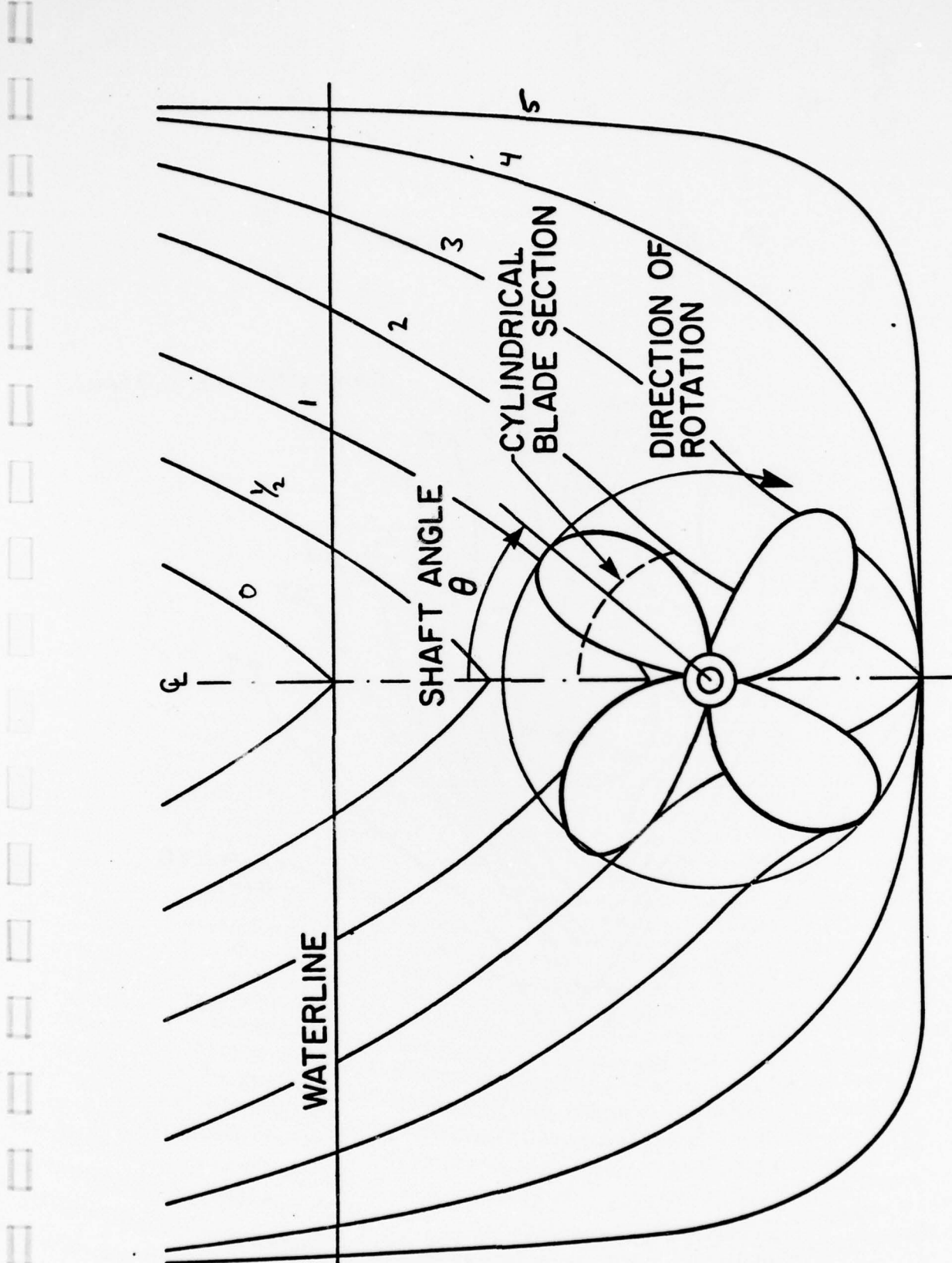


FIGURE 1. SCHEMATIC VIEW OF PROPELLER PLANE OF SINGLE SCREW MERCHANT VESSEL.

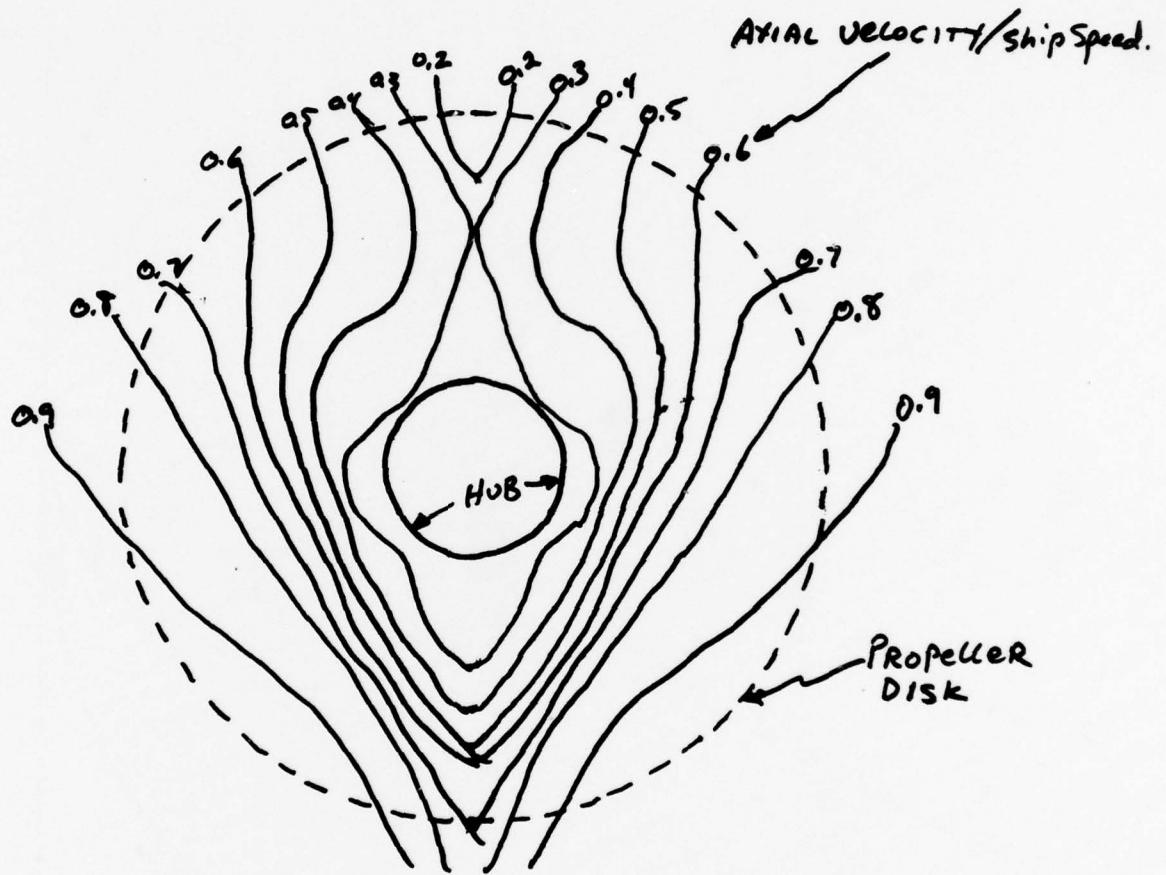


FIGURE 2. ISOVELOCITY WAKE CONTOURS FOR AXIAL VELOCITY
IN PROPELLER PLANE OF "TYPICAL" MERCHANT
VESSEL.

NOTE: ANGLE OF ATTACK α FLUCTUATES
DUE TO VARIATIONS IN AXIAL INFLOW
VELOCITY V_x , CAUSING CHANGES IN
CAVITY VOLUME

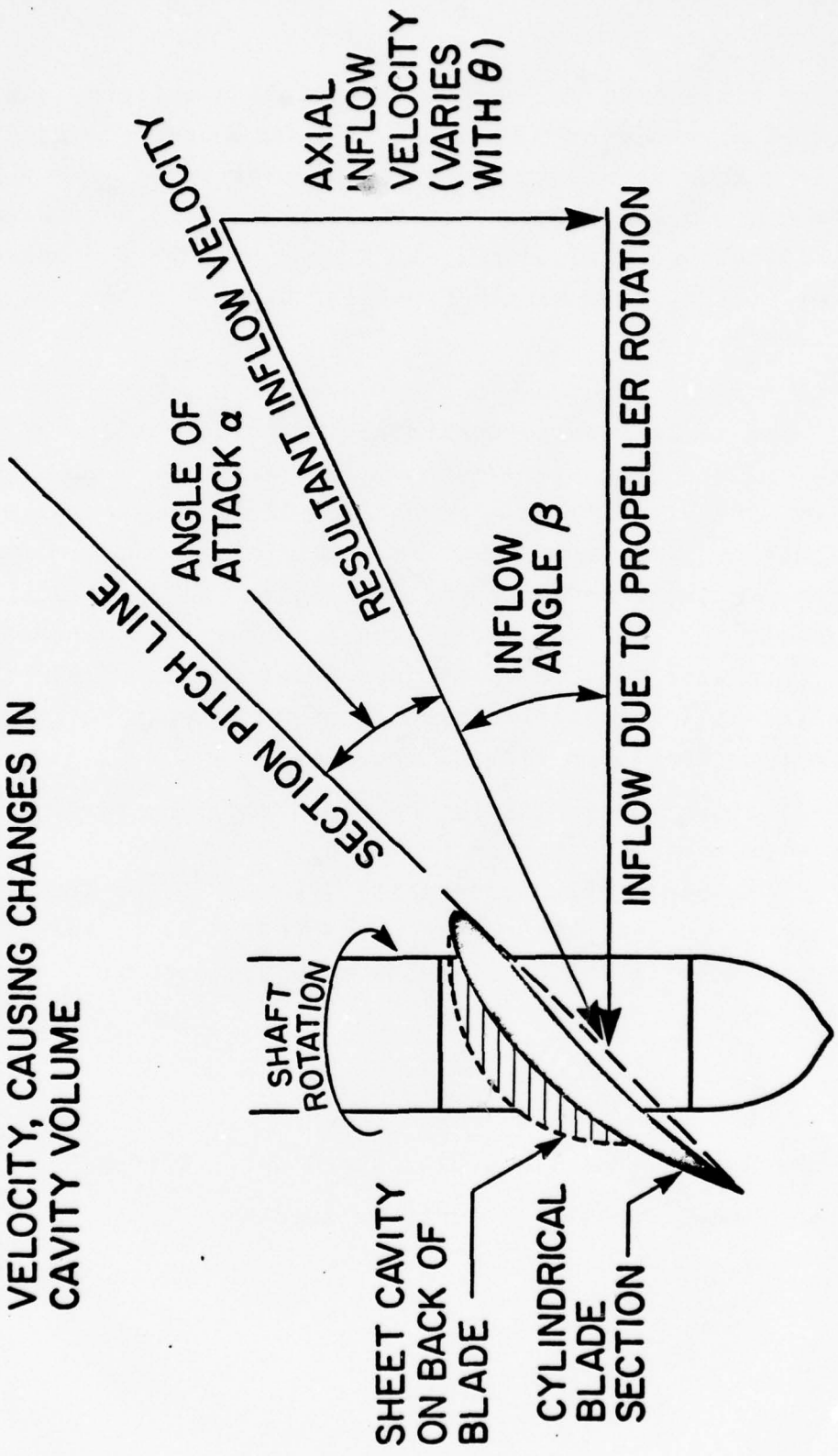


FIGURE 3. SCHEMATIC OF PROPELLER BLADE SECTION INFLOW GEOMETRY.

power. Figure 4 presents the observed cavitation patterns and relevant propeller and ship data as taken from these references. Both propellers show cavitation in the region of small wake velocities. The maximum sheet cavity on these propellers covers approximately 10% of the blade surface. Figure 5 shows the measured cavity volume history on a single propeller blade for the ore carrier propeller [5].

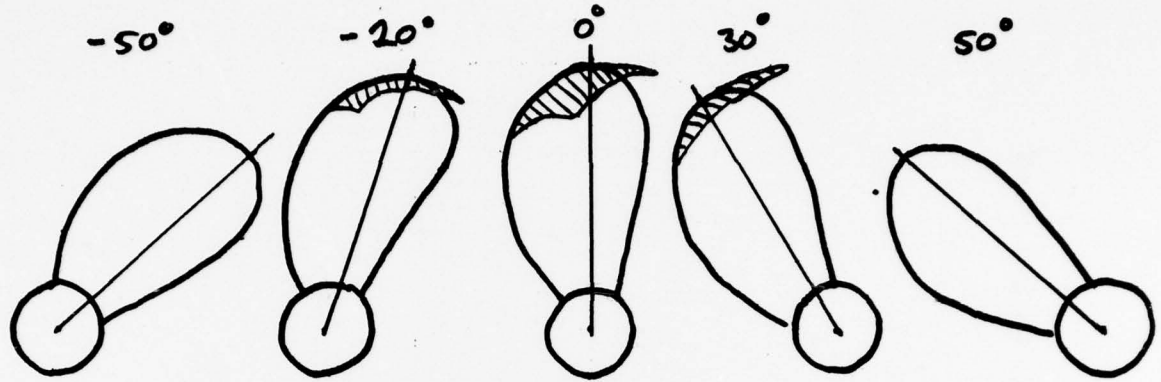
The amount of unsteady cavitation on a given propeller in a non-uniform wake is limited by considerations of propeller efficiency, erosion, and ship vibration [6]. In order to reduce the intensity of cavitation on a given propeller, the propeller blade area must be increased, which implies a reduction in propeller efficiency and an increase in propeller weight. If the blade area is reduced, the unsteady cavitation increase will cause an increase in ship vibration and propeller erosion. The most efficient propeller will "evolve" to have as much unsteady cavitation as vibration considerations will allow.

Ship hull vibration is limited by structural and personnel acceptability criteria. Assuming that a typical vessel is "modally dense" at the blade rate frequencies [7], the power input to hull vibration per unit drive force is the real part of the impedance. Approximating the ship impedance at blade rate frequencies as a finite beam [8]:

$$\frac{V^2}{F^2} = \frac{\pi}{M} \frac{\Delta N}{\Delta \omega} (1+i) \quad (2.1)$$

where M is the driven mass (including added mass effects)

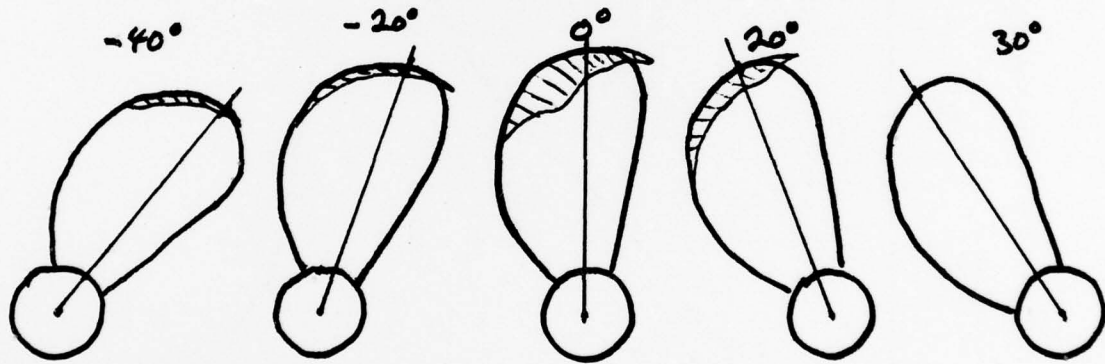
$\frac{\Delta N}{\Delta \omega}$ is the modal density per unit bandwidth



FULL SCALE CAVITATION OBSERVED ON

250,000 DWT TANKER [3]

PROPELLER: 29' DIAMETER EAR = .57
5 BLADES RPM = 85.
32000 S.H.P.



FULL SCALE CAVITATION PATTERNS OBSERVED ON

224,000 DWT ORE CARRIER: BALLAST CONDITION [4]

PROPELLER: 22' DIAMETER EAR = .61
5 BLADES RPM = 103
31,000 S.H.P.

FIGURE 4. SHEET CAVITATION PATTERNS OBSERVED ON FULL SIZE SHIP PROPELLERS

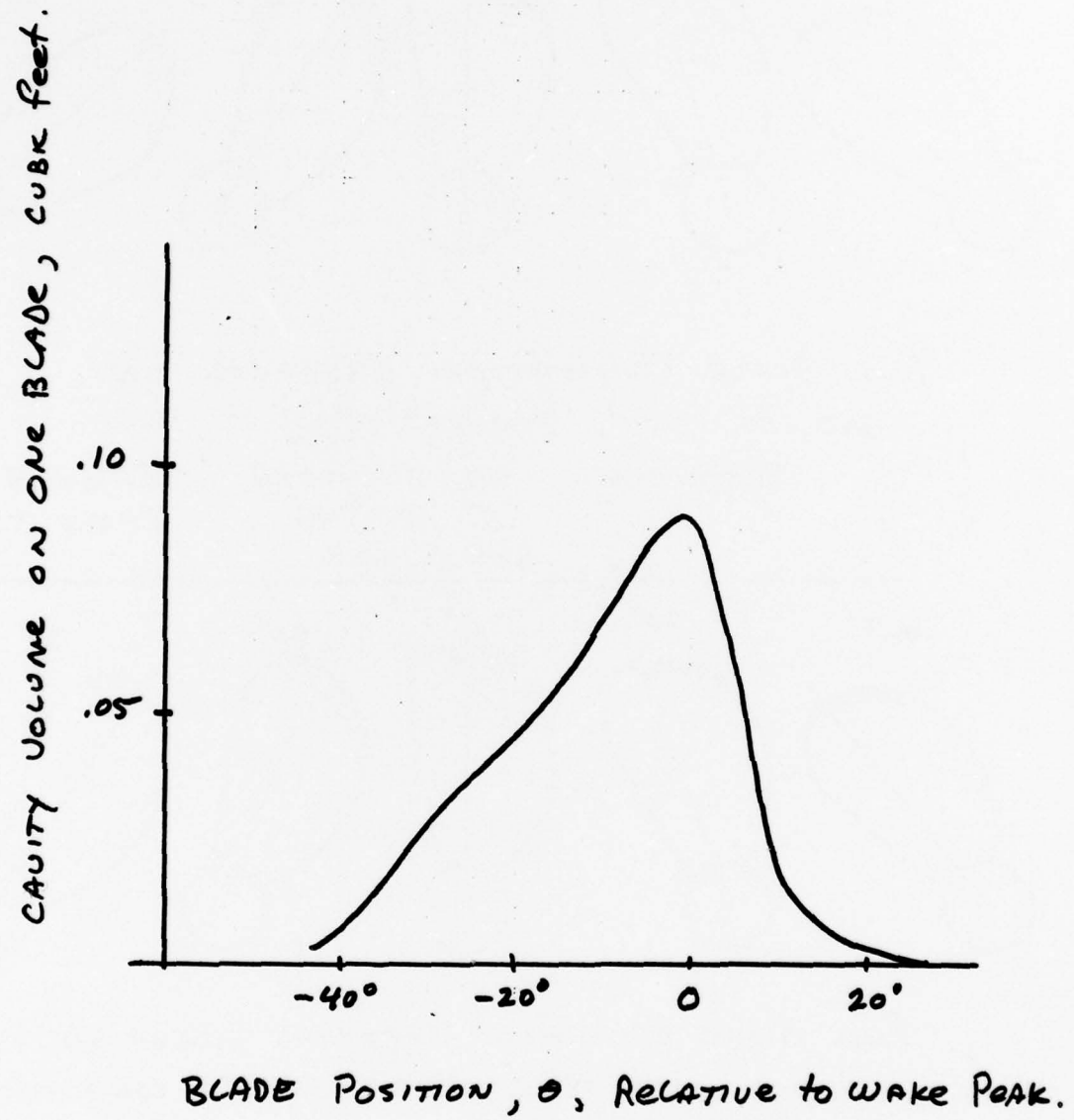


FIGURE 5. MEASURED CAVITY VOLUME HISTORY ON SHIP PROPELLER [5].

Since ship vibration criteria [9] limit the maximum structural velocities, these criteria are essentially limits on the drive point velocity (stern vibration). Thus, the relationship 2.1 also defines the velocity per unit force, and the modal density can be approximated by its limiting value

$$\frac{\Delta N}{\Delta \omega} \sim \frac{C_B \cdot L}{2\pi} \quad (2.2)$$

where C_B is the bending wave speed.

For geometrically similar ships of length L , which meet the same vibration criteria, the allowable excitation force at a given frequency (blade rate) will vary with ship size as:

$$F^2 \sim \frac{M}{C_B \cdot L} \sim \frac{L^3}{L^{\frac{1}{2}} \cdot \omega^{\frac{1}{2}}} \sim L^{5/2}. \quad (2.3)$$

From a survey of ship population characteristics, it was determined (see Sec. 3) that propeller diameter (D) and length were approximately related as:

$$D \sim L^{7/5}. \quad (2.4)$$

or, $F^2 \sim D^{10/3} \approx D^3. \quad (2.5)$

Thus, one may conclude that the allowable source strength due to cavitation may increase as the cube of the propeller diameter to achieve similar vibration levels at blade rate frequencies on geometrically similar ships. Note that if one uses the same propeller design criteria, independent of ship scale, then the resulting unsteady cavitation volume will, in fact, vary as diameter cubed.

Unfortunately, ships are not "geometrically similar" as scale increases. Typically, ships become less rigid as they become larger, and hence the modal density will increase faster

than the square root of length. Hence, one would correctly expect larger vessels with propellers designed by the same criteria to suffer more from vibrational problems [10].

2.3 Radiation from Cavity Volume Changes

Since at the frequencies of interest (6-10 Hz), the propeller size is much smaller than an acoustic wavelength, changes in the cavity volume with time will radiate directly as a simple volume source (monopole) located below a pressure release surface. If the cavity volume ($V(\theta)$) time history on one propeller blade (see figure 5) is represented as it's fourier series,

$$V_1(\theta) = \sum_{n=0}^{\infty} a_n e^{in\theta} \quad (2.6)$$

and the volume on the b^{th} blade will be

$$V_b(\theta) = \sum_{n=0}^{\infty} a_n e^{in(\theta + \frac{2\pi b}{B})}. \quad (2.7)$$

Then the total volume on a propeller of B blades will be:

$$\begin{aligned} V_T(\theta) &= \sum_{n=0}^{\infty} \sum_{b=1}^{\infty} a_n e^{in(\theta + \frac{2\pi b}{B})} \\ &= \sum_{n=0}^{\infty} a_n e^{in\theta} \cdot \sum_{b=1}^{\infty} e^{in(\frac{2\pi b}{B})} \end{aligned} \quad (2.8)$$

The first summation is identically the volume history on the index blade and the second term has non-zero values only for n equal to multiples of B , where the value of the summation is B . Thus, only frequencies equal to multiples of the number of blades (B) will exist; and the amplitude of the harmonics of the total cavity volume history will be simply the B times the B^{th} order of harmonics of the cavity volume history on a single blade.

Since the rotation angle θ and time t are directly related by the rotational speed of the propeller with the frequency of rotation (ω)

$$v_p(t) = \sum_{n=0}^{\infty} A_n e^{in\omega t}, \quad n=B, 2B \dots \text{ and } A_n = B \cdot a_n \quad (2.9)$$

The source strength of the radiation from a propeller volume history can be given then as

$$P_o = \frac{1}{r} \rho_0 \pi f_n^2 A_n. \quad (2.10)$$

However, if the single blade volume history occurs in an interval of propeller revolution less than $2\pi/B$, and the volume history is not too non-sinusoidal, then the fundamental harmonic of blade rate can be approximated as

$$A_N \sim \frac{V_{max}}{2} \quad (2.11)$$

where V_{max} is the maximum volume on a blade during a revolution. Thus, the mean squared pressure radiated from this monopole source in an unbounded medium at the fundamental blade rate frequency is approximately:

$$P_o^2 \approx \left(\frac{\pi f_o^2 \rho_0 V_{max}}{2\sqrt{2} r} \right)^2. \quad (2.12)$$

The proximity of the free surface introduces an image which impairs the radiation over the frequencies of concern.* The pressure radiated out an angle ϕ from this source at depth H below the free surface is:

$$P^2(\phi) = 2P_o^2 [1 - \cos(2K_T H)] \quad (2.13)$$

*It is assumed that the vessel hull does not affect the average pressure radiated by this volume source. This effect is presently under investigation.

or approximately:

$$P_d^2 = \frac{P_o^2(\phi)}{\sin^2\phi} \sim 4P_o^2(KH)^2 \quad (2.14)$$

where P_d^2 = dipole source strength, which is equivalent to the mean square pressure radiated at a depression angle (ϕ) of 90° .

Rewriting into one equation:

$$P_d^2 = \left(\frac{8\pi^2 P_o}{2\sqrt{2} r \cdot c} \cdot f_B^3 \cdot H \cdot V_{max} \right)^2 \quad (2.15)$$

For radiation referenced to a 1 meter range, the mean squared pressure in dB referenced to a dynes/cm² is:

$$10 \log[P_d^2] / \mu\text{bar} \times \text{meter} = 10 \log[0.73 f^6 \cdot H^2 \cdot V_{max}^2] \quad (2.16)$$

where H = source depth in feet and

V_{max} = maximum cavity volume per blade in feet³.

Note that to characterize the source strength from propeller cavity volume modulation, one must either specify the monopole source strength (P_o^2) and the source depth (H); or the dipole source strength (P_d^2). For completeness, and for the convenience of the user, we have presented the source strength model of merchant vessel blade rate radiation as both a dipole source strength and as a monopole source strength at a given depth, with the depth of the source assumed to be equal to the ship draft minus 85% of the propeller diameter. The dipole source strength represents the *net pressure* radiated by the volume source and its surface image. This representation is convenient in that a single number is sufficient to characterize the net acoustic radiation from a given vessel's propeller. The monopole source strength represents the pressure that would be radiated by the volume source in an infinite medium. Since there in fact exists a nearby free surface, the depth of

this monopole source below this free surface must also be included to accurately characterize the acoustic radiation. Because most existing ambient noise prediction schemes use this latter description, the model developed below is also expressed as a monopole source strength and source depth. Note, however, that the conversion to dipole source strength is straight forward (Eq. 2.14).

2.4 Harmonics of Blade Rate

The higher harmonics (n) of blade rate will be governed by the higher harmonics ($B \cdot n$) of the cavity volume history. Prediction of these harmonics requires detailed and accurate information of the volume pulse pitch width, cavity growth and collapse rates, and may well be limited by natural cavity dynamics. A discussion of some limits on the cavity volume acceleration is presented in ref. 11. For this interim model, an empirical collapse of existing data [12, 13] is used. Figure 6a shows this data, normalized to the second harmonic of blade rate. Figure 6b shows the relationships assumed for this interim model for harmonics of blade rate. The source level of the harmonics are expressed relative to the level of the fundamental blade rate. Both monopole and dipole models are shown. Note that the data from [13] is at variance with this assumed relationship. This difference is *speculated* to be due to reradiation from excited hull vibration which may augment the direct radiation for very large vessels at low frequencies.

3.0 ESTIMATION OF MERCHANT SHIP SOURCE STRENGTHS

3.1 Design Limitations for Maximum Unsteady Cavity Volumes

The maximum unsteady cavity on four-bladed marine propeller would occur in a wake where a blade is completely cavitating in the 0° position, and cavitation free in the 45° and 315° positions. The total cavity volume history on the propeller would then look

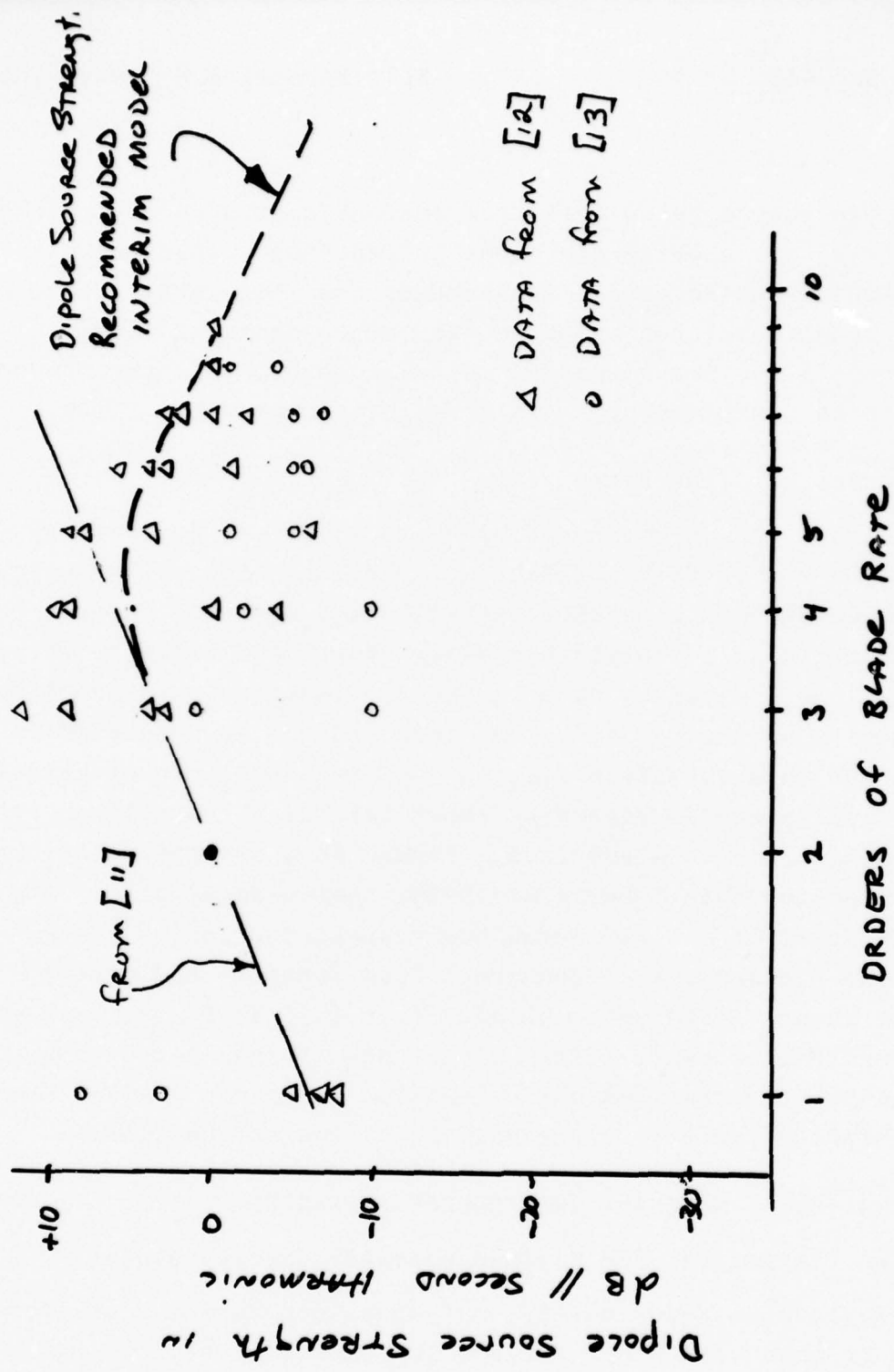


FIGURE 6a. RELATIONSHIP OF HIGHER HARMONICS OF BLADE RATE TO FIRST AND SECOND HARMONICS [11, 12, 13].

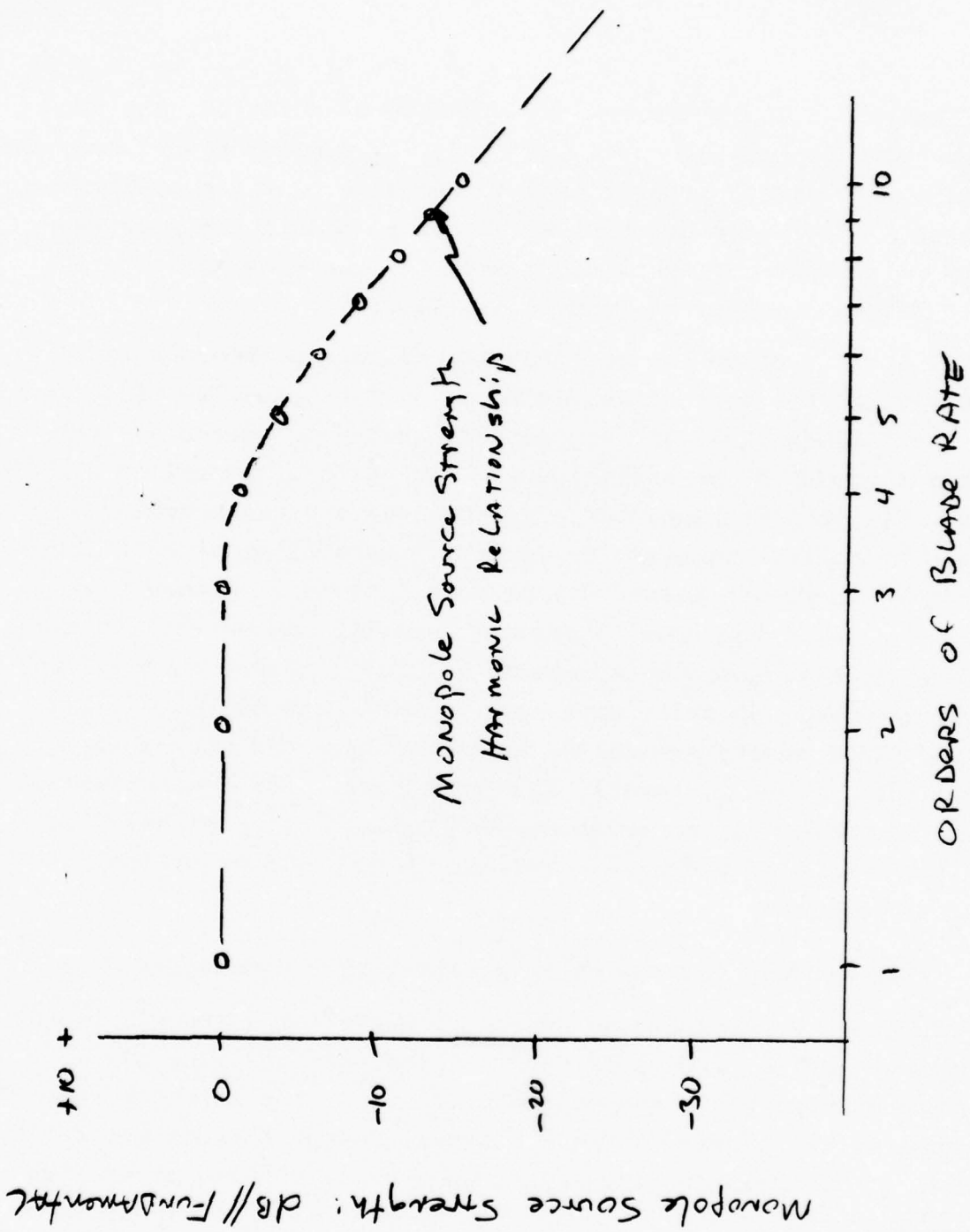


FIGURE 6B: HARMONIC RELATIONSHIP TO FUNDAMENTAL BLADE RATE LEVEL

like figure 7. It is assumed that in this 0° position, the propeller blade is heavily cavitating and, for similar propellers, the cavity volume is proportional to the cube of the propeller diameter. Figure 8 presents the calculated relationship between cavity volume and cavity planform area for cambered marine propeller blades as obtained from refs. [11, 14].

If it is further assumed that the maximum planform area of the cavity at the 0° position is equal to the propeller blade area, then the maximum limit to the unsteady cavity volume on a given propeller blade can be estimated as a function of propeller diameter. Figure 9 presents these relationships between cavity volume and propeller diameter for various intensities of cavitation. Also shown in figure 9 are several observations of either cavity area or volume taken from literature [3,4,5], and several volumes inferred from acoustic measurements [12, 13]. Based on these observed or inferred cavity areas and volumes, the curves of 30%, 10% and 3% of cavity area/blade area have been designated for convenience as heavy, normal, and light cavitation respectively. Again, the upper curve represents the maximum to be expected for an extreme case of propeller cavitation and would be unlikely to occur in practice.

3.2 Relationship to Obtainable Merchant Ship Parameters

In order to predict the source strength for a vessel without knowing the actual propeller cavity volume history, one must make assumptions about the characteristics of the merchant ship population. We assume, quite arbitrarily, that the maximum cavity volumes at design ship speed found on propellers of a given size are distributed normally around the "normal" line of figure 9, with the "heavy" and "light" cavitation levels equal to two standard deviations from this "normal" volume relationship.

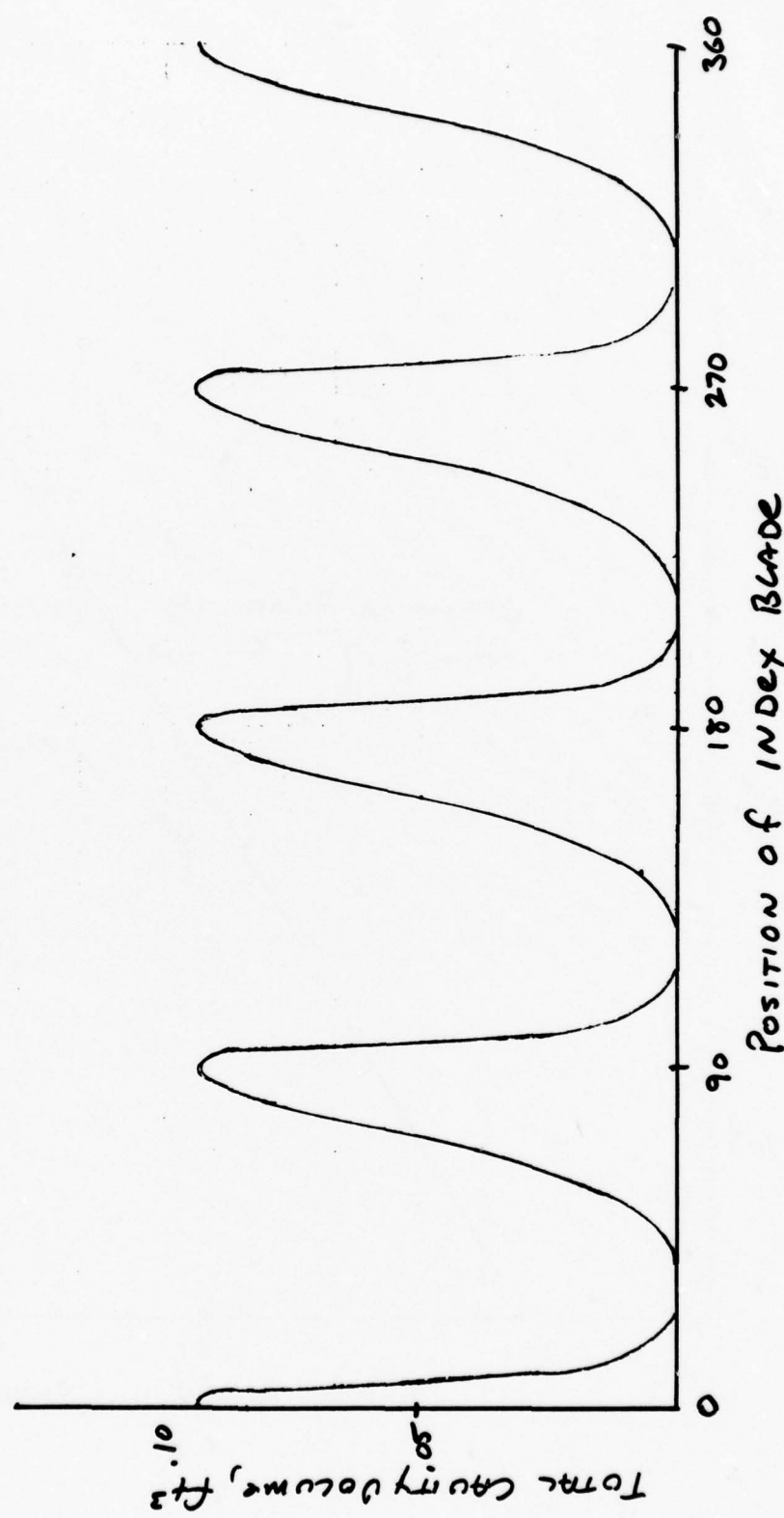


FIGURE 7. TOTAL CAVITY VOLUME HISTORY ON FOUR BLADED PROPELLER [5].

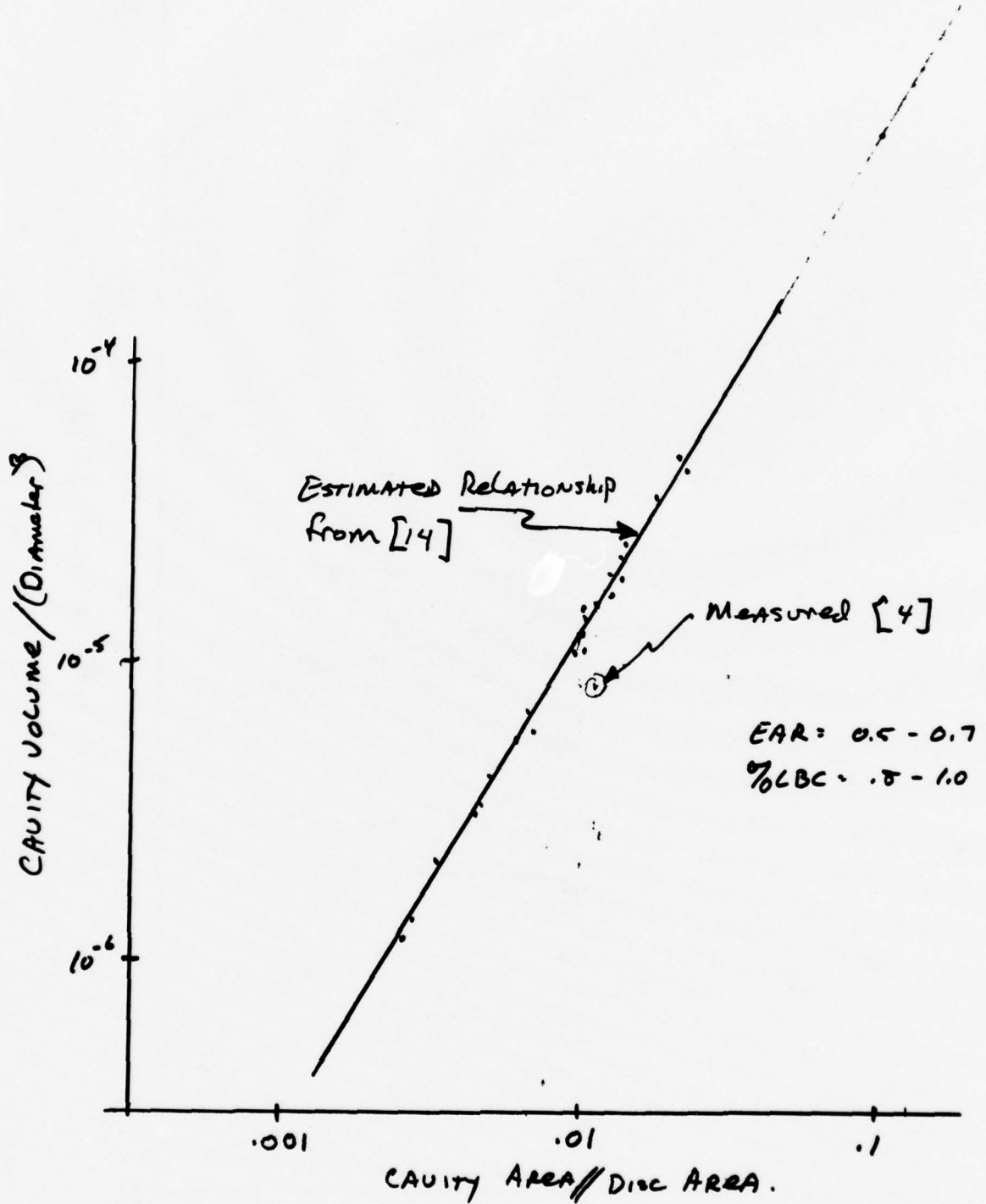


Figure 8: CAVITY VOLUME & AREA RELATIONSHIPS
FOR CAMBERED FOILS IN SHIP WAKES.

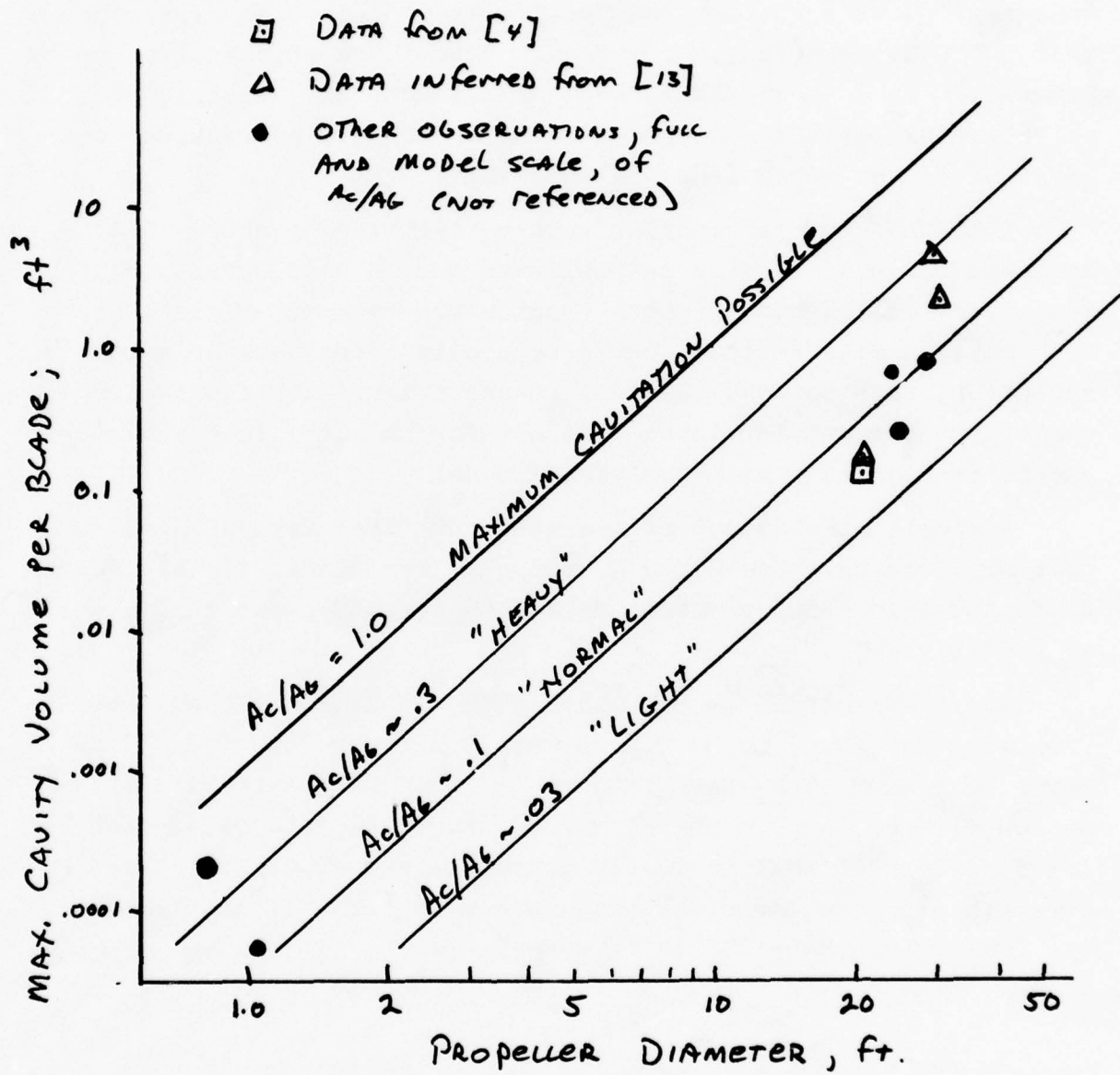


FIGURE 9. MAXIMUM CAVITY VOLUMES OBSERVED ON MODEL AND FULL SCALE PROPELLERS.

The basis for this assumption (see Section 2) is that propellers designed to have very light cavitation, even in the extreme wake region, will be less than optimally efficient and therefore, will not tend to occur in practice. Propellers which suffer heavy cavitation in a single screw wake will induce ship vibrations which are excessive; and the "design" speed will be reduced to a point where the vibrations are tolerable.

Note that this assumption must be verified by data. Both acoustic and non-acoustic measurements may be used. The use of non-acoustic measurements both expands the base of available data and provides data uncontaminated by possible unknowns in acoustic radiation, such as possible hull re-radiation. The few available observations shown in figure 9 do not form a sufficient basis for the derivation of a high confidence model.

A sample population* of the merchant fleet was surveyed to determine the relationship between propeller diameter, ship design draft and ship length. These relationships are shown in figures 10 and 11.

For the same sample population, the fundamental blade rate frequency was found to be approximately independent of any diameter or length parameter. Figure 12 shows the observed distribution for the sampled population of the fundamental blade rate frequency. Note that it is now possible to express the source strength of propeller blade rate solely in terms of ship length (in feet) for a "normal" or "average" vessel, at its design speed i.e.

* Approximately 50 ships were found in naval engineering journals where sufficient information on the propeller design was included. An attempt was made to keep this sample representative of the age and length distributions of the world fleet population.

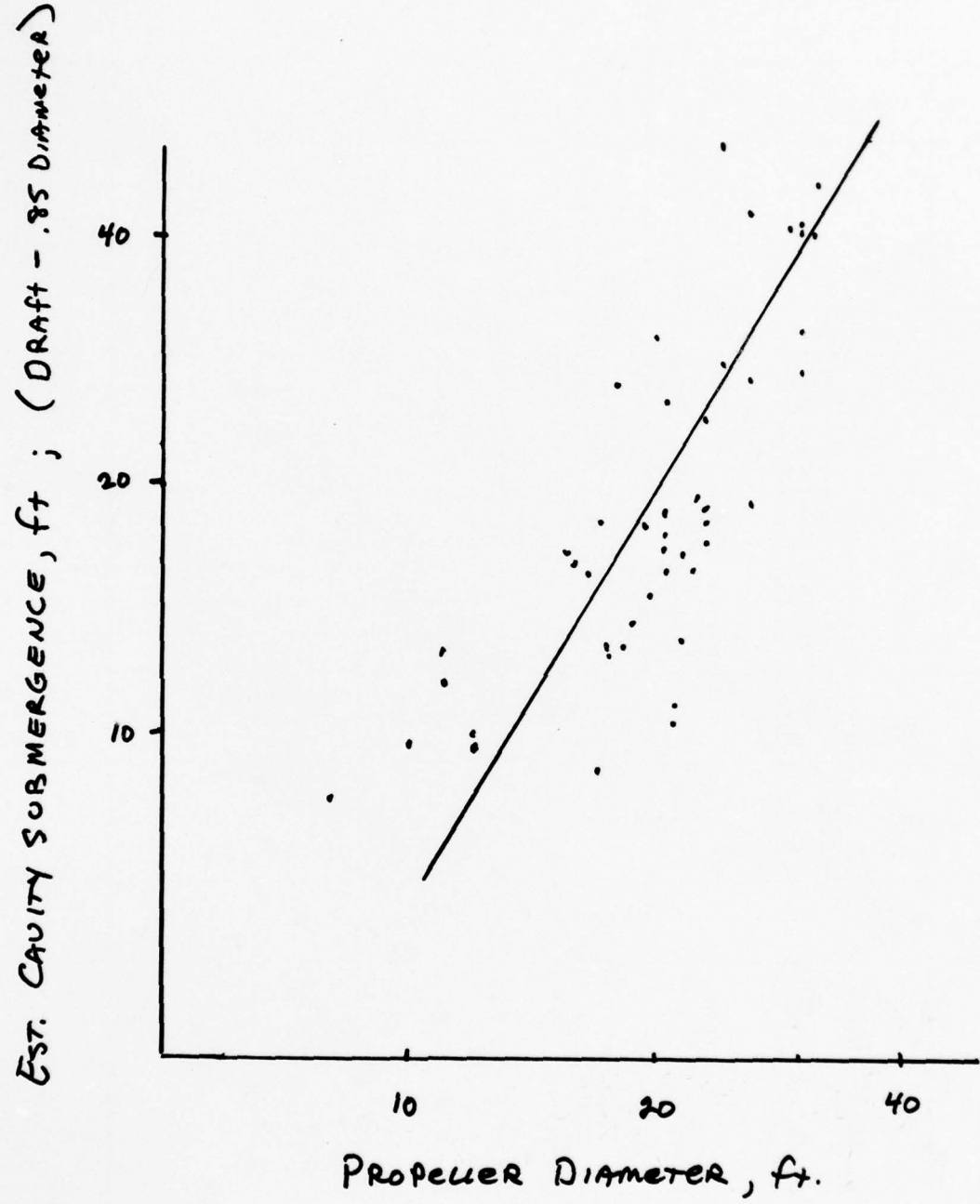


FIGURE 10. ESTIMATED PROPELLER CAVITY SUBMERGENCE FOR SAMPLE FLEET POPULATION.

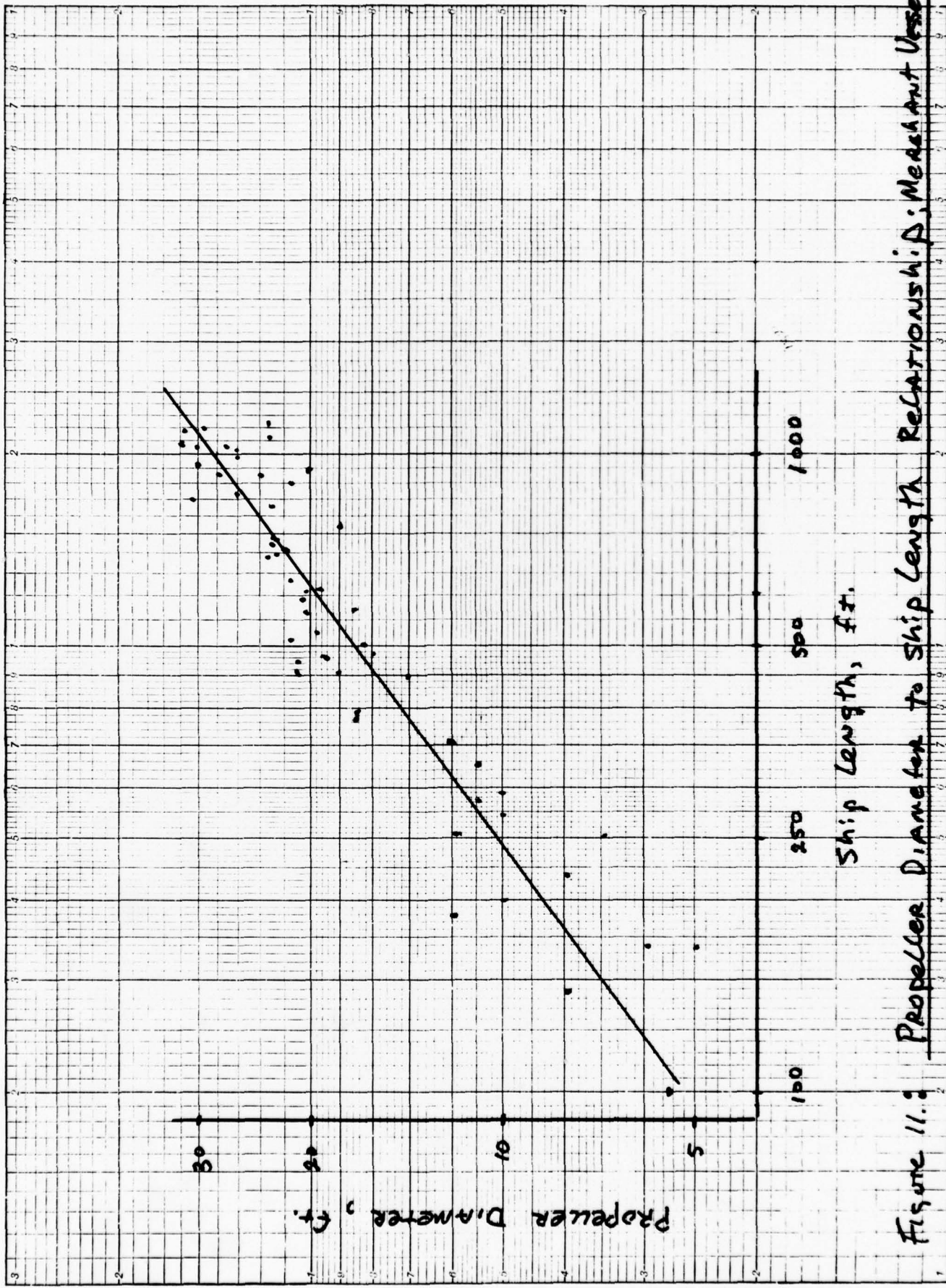


Figure 11.3 Propeller Diameter to Ship Length Relationship; Merchant Vessels

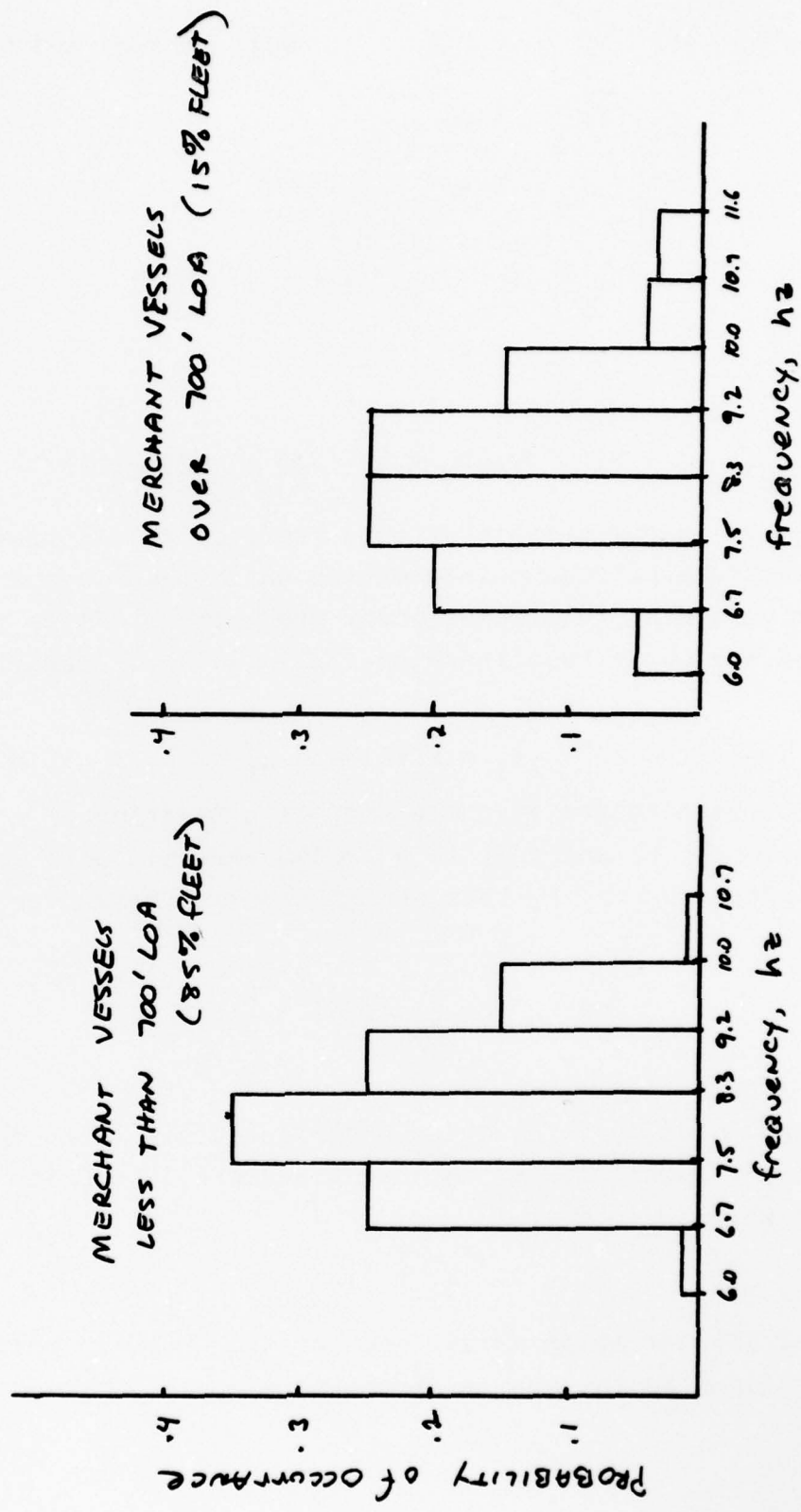


FIGURE 12. ESTIMATED DISTRIBUTION OF BLADE RATE FREQUENCY FOR THE WORLD FLEET OF MERCHANT VESSELS.

$$V = 3 \times 10^{-5} \cdot D^3 \quad (3.1)$$

$$H = .12 D^{1.7} \quad (3.2)$$

$$D = .16 L^{.75} \quad (3.3)$$

$$f = 8 \text{ Hz} \quad (3.4)$$

Therefore,

$$10 \log(P_d^2) // \mu P_a \times m = -30 + 70 \log(L) \quad (3.5)$$

However, in our pursuit of this "normal" relationship, we have neglected significant information which describes the deviation from this mean relationship for the merchant fleet population. If each of the above relationships (3.1 - 3.4) is characterized as:

$$x_i = \bar{x}_i(L) + \delta x_i \quad (3.6)$$

where $\bar{x}_i(L)$ is a random variable that is a function of another random variable, L; and δx_i is a random variable with zero mean that is independent of L, then we can express the source strength as:

$$\log(P_D^2) = \sum_i \bar{x}_i(L) + \sum_i \delta x_i \quad (3.7)$$

Furthermore, if δx_i is normally distributed with zero mean and variance σ_i^2 , then: $\sum_i \delta x_i$ is normally distributed with zero mean and variance:

$$\sigma^2 = \sum_i \sigma_i^2 .$$

Thus, the variation around each of the "normal" relationships can be included in the source strength, i.e.

$$10 \log V = -45 + 30 \log D + 10 \log \delta_{V//D} \quad (3.8)$$

$$10 \log H = -9.2 + 17 \log D + 10 \log \delta_{H//D} \quad (3.9)$$

$$10 \log D = -8 + 7.5 \log L + 10 \log \delta_{D//L} \quad (3.10)$$

$$10 \log f = 9 + 10 \log \delta_f \quad (3.11)$$

Where for example, the function $\delta_{V//D}$ is the conditional variation of the cavity volume, given a propeller diameter. This conditional variation is assumed to be describable as a normal distribution with a zero mean value and variance, $\sigma^2_{V//D}$. For the sample population surveyed (and the arbitrary assumption on the volume to diameter relationship), these conditional deviations in percent of the mean value are given in Table 1. Note then that the logarithm of these relationships satisfy the conditions of independence and one can express the dipole source strength as:

$$SL_D = -30 + 70 \log L + 10 \log \delta_{SL//L} \quad (3.12)$$

where $\delta_{SL//L}$ is the uncertainty in source level which is characterized by its variance (see Eq. 2.16):

$$\sigma^2_{SL//L} = (\sigma^2_{V//D})^2 + (\sigma^2_{H//D})^2 + (\sigma^2_{D//L})^{9.4} + (\sigma^2_f)^6 \quad (3.13)$$

Thus for the sample ship population surveyed and for the assumptions made regarding this population, the variation around the "normal" relationship given above is characterized by a standard deviation, σ_t , equal to 11 dB. Note for example, that if one knows the ship propeller diameter (rather than just length), the uncertainty in the source level is significantly reduced. For this case,

$$SL_D = 44 \times 94 \log D + 10 \log \sigma_{SL//D} \quad (3.14)$$

and the standard deviation of the uncertainty, $\sigma_{SL//D}$ is only 8 dB.

TABLE 1: APPROXIMATE CONDITIONAL STANDARD DEVIATION (σ) OF SAMPLE SHIP POPULATION

	<u>% Mean Value</u>	<u>$10 \log(\sigma)$: dB// Mean Value</u>
$\sigma_{V//D}$	500	7.0
$\sigma_{H//D}$	150	1.76
$\sigma_{D//L}$	130	1.14
σ_f	120	0.8

3.3 Model for the Dipole Source Strengths of Blade Rate for the World's Merchant Fleet

The 1972 merchant fleet was surveyed [15] to determine the probability density function (PDF) for occurrence of ships at sea of various lengths. These data were manipulated based on estimated duty cycles as a function of ship size and type to yield the distribution shown in figure 13. Note that this PDF for ship length can be mapped by Eq. 3.12 into a PDF for the occurrence of blade rate source levels for "normal" ships. The effect of the uncertainty in the source level, given a ship length ($\delta_{SL//L}$), (which is by definition a normally distributed PDF which is independent of the source level), on the resulting probably distribution of source level can be included by simply convolving the two density functions:

$$PDF_{SL} = PDF_{SL//L} * \delta_{SL//L} . \quad (3.15)$$

Because of the apparent strong dependence of blade rate source strength on ship size, this distribution of vessels is treated as two separate groups. This allows a more detailed analysis of the "noisier" (larger) vessels. In addition, the operational behavior of larger vessels is somewhat different from the general fleet. Figure 14 and 15 present the estimated dipole source strength PDF's for these two groupings of merchant vessels. (The PDF for blade rate frequency is shown in figure 12.)

For the set of merchant vessels less than 700 feet in length, the dipole source strengths at blade rate are estimated to cover a range of 80 dB, with a mean value of 155 dB and a standard deviation of 17 dB. For the set of vessels over 700 feet in length, the source levels at blade rate are estimated to cover a range of 50 dB with a mean value of 172 dB and a standard deviation of 9.2 dB. The shape of the PDF for these larger merchant vessels is

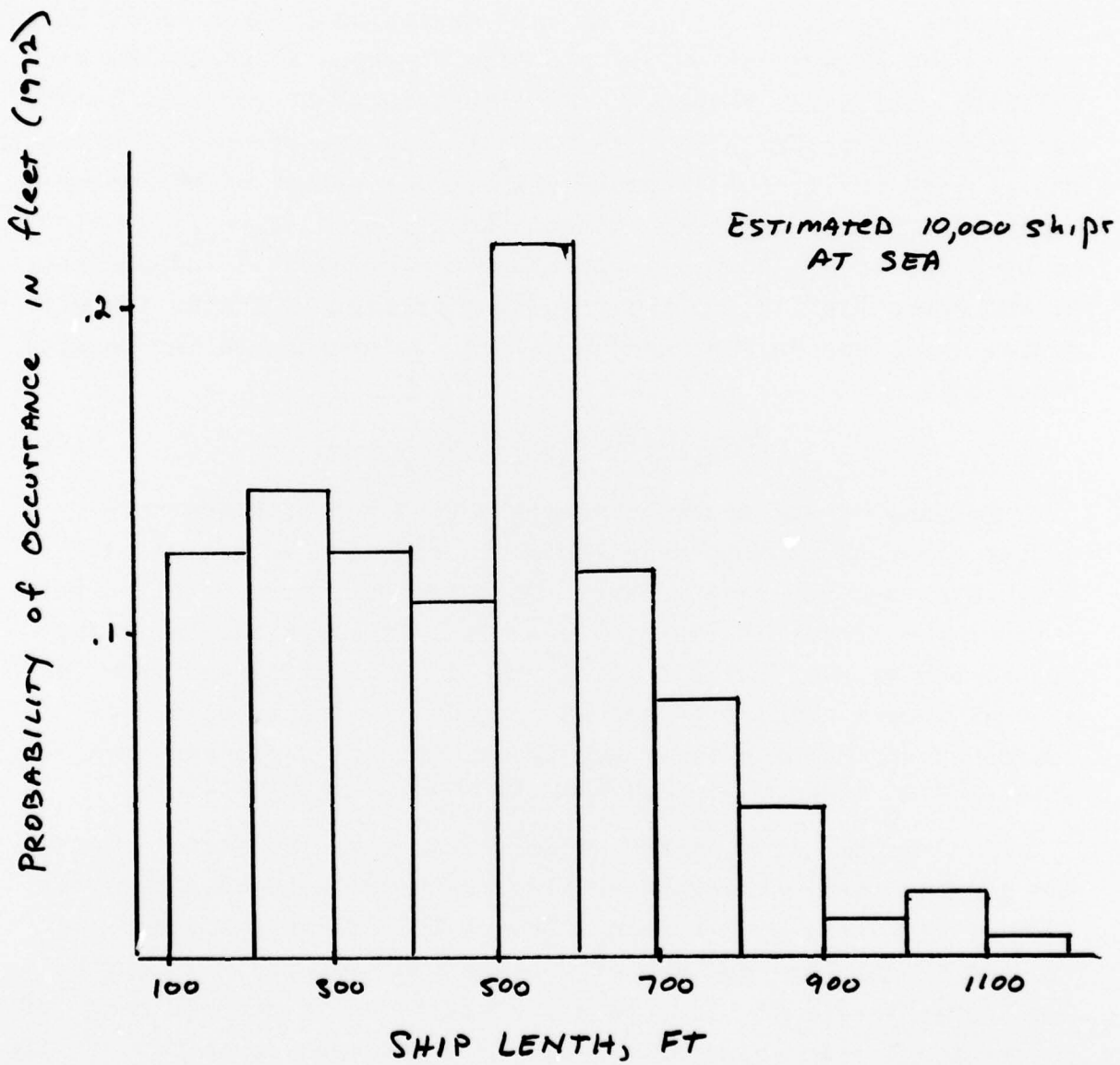


FIGURE 13. ESTIMATED DISTRIBUTION OF SHIP LENGTH FOR THE WORLD FLEET OF MERCHANT VESSELS (1972).

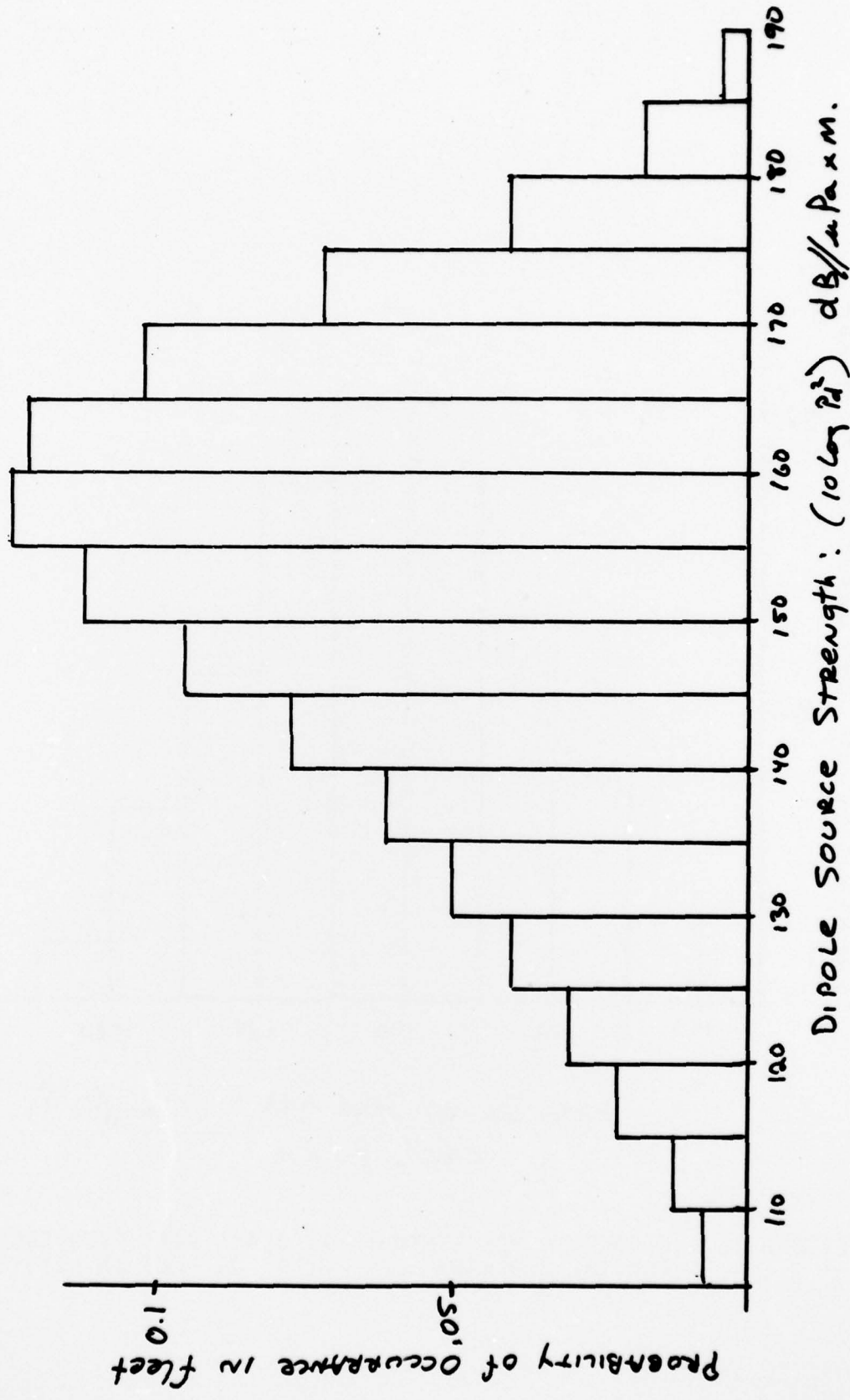
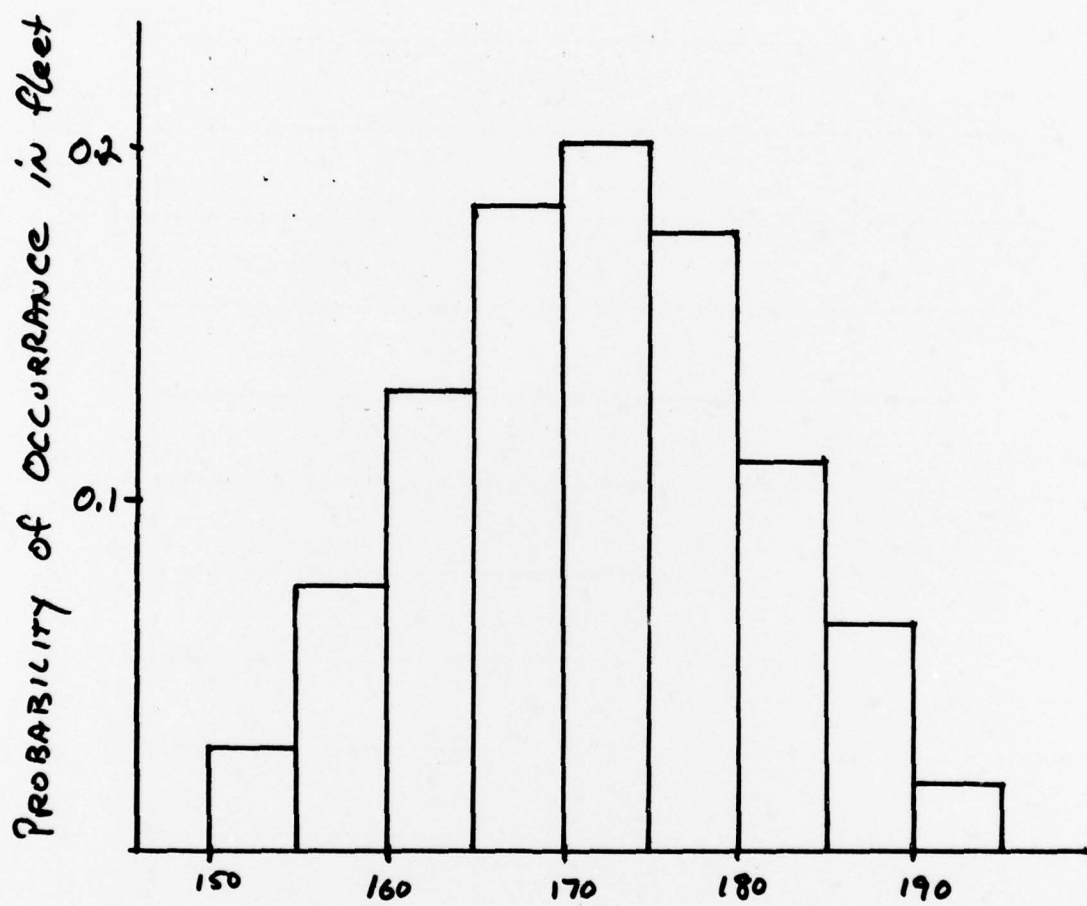


FIGURE 14. DIPOLE SOURCE STRENGTH AT BLADE RATE FREQUENCY FOR THE MERCHANT FLEET LESS THAN 700 FEET IN LENGTH.



Dipole Source Strength : $(10 \log(P_d^2))$
 $\text{dB}/\mu\text{Pa} \times \text{m}$

FIGURE 15. DIPOLE SOURCE STRENGTH AT BLADE RATE FREQUENCY FOR THE MERCHANT FLEET OVER 700 FEET IN LENGTH.

dominated by the uncertainty term of equation 3.1 while the PDF shape for the smaller vessels is dominated by the conditional source level mapping from the PDF of ship lengths.

Note that these PDF's represent the expected distribution for blade rate dipole source strength for the merchant fleet operating at *design speed*. These source levels and frequencies will be severely affected by a general reduction in vessel speed, as has recently occurred due to energy consideration. Calculations of [11] show a decrease of 1 dB in expected source level for each 1% speed reduction of a typical ship.

3.4 Model for the Monopole Source Strengths and Source Depths of Merchant Fleet Blade Rate

Following the same procedure as section 3.2, it can be shown that the monopole source strength (eq. 2.12) is related to propeller diameter (D) to ship length (L) (in feet) as:

$$10 \log [P_o^2] \text{dB}/\mu\text{Pa} \times m = 95 + 60 \log D \quad (3.16)$$

or

$$10 \log [P_o^2] \text{dB}/\mu\text{Pa} \times m = 47 + 45 \log L \quad (3.17)$$

The estimated source depth (H) can also be related to ship length by Eq. 3.2 and 3.3 e.g.:

$$H = .0053 L^{1.28} \quad (3.18)$$

Note, then, that the monopole source strength ($10 \log P_o^2$) and the source depth are both dependent on ship size and are *not* independent; i.e. the cavitation volume source on larger vessels will be both more intense and located at a deeper submergence.

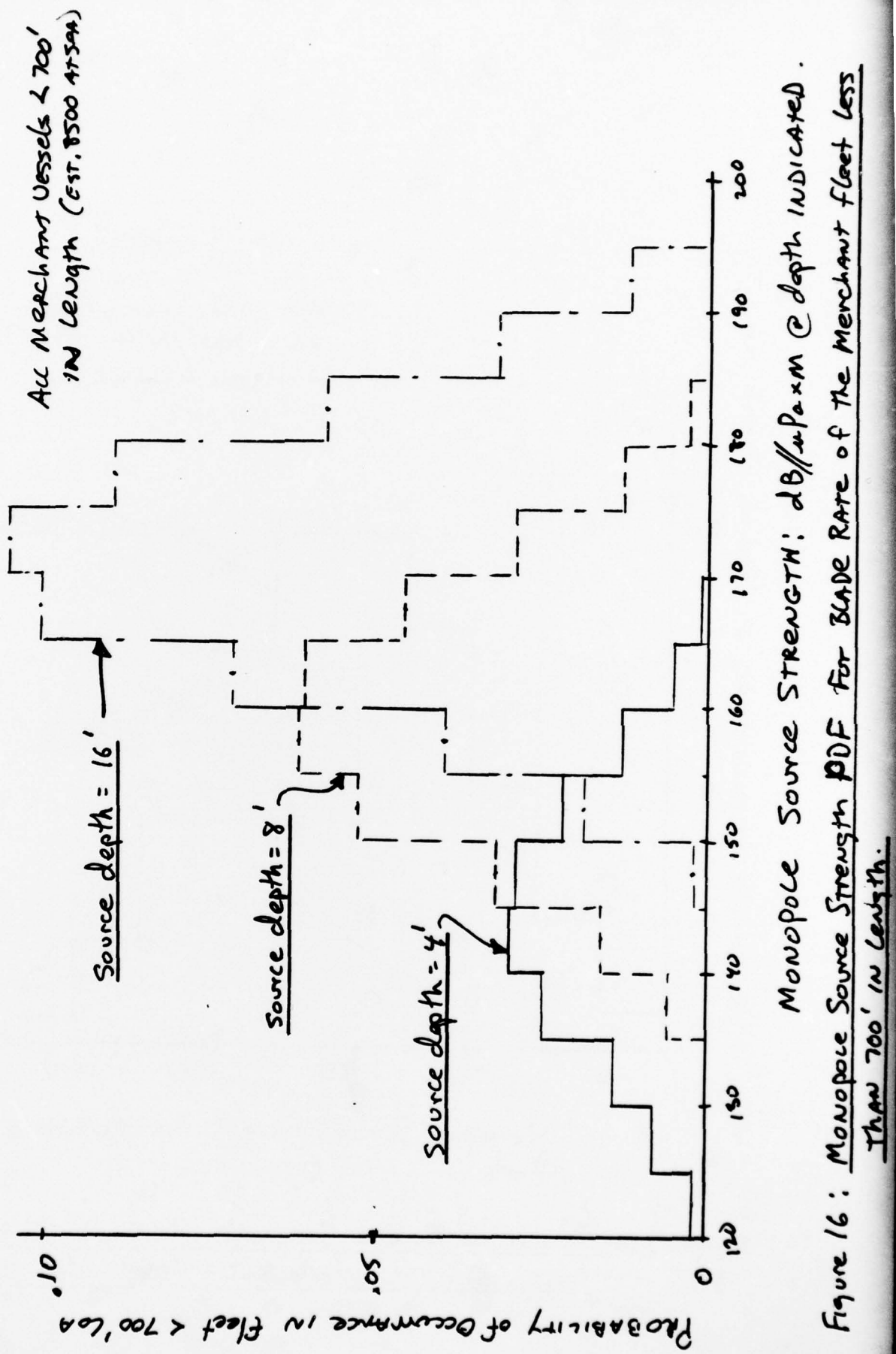
In addition, the deviation from these mean relationships for monopole source strength (Eq. 3.16-3.18) must be included to obtain a description of the probability of occurrence of the source strength and source depth. The resulting probability density function (PDF) for source strengths in the world fleet is then 3-dimensional, i.e. the probability of occurrence of a given source level also depends on source depth.

In order to present these PDF's in a readily usable fashion, we have divided the distribution of source depths for the world's fleet into "bands" of depth centered at intervals, selected to be octaves apart. Figures 16 and 17 present the estimated PDF's for the monopole source strengths at blade rate as a function of source depth. (Note that the world fleet is subdivided into two groups based on ship length as described in section 3.3). Figure 16 shows the estimated PDF for blade rate of vessels less than 700 feet in length, for source depths of 4, 8, and 16 feet. Figure 17 presents the source strength for vessels over 700 feet in length, which have an assumed source depth of 32 feet. Note that these distributions in conjunction with Eq. 2.14 will yield the PDF's of figures 14 and 15.

4.0 CONCLUSIONS AND RECOMMENDATIONS

The model presented for the source strength of propeller blade rate is based on the physics of propeller cavitation in non-uniform wakes and on observations of cavitation volume histories obtained from models and full scale propellers. These observations include optical measurements of cavity volume histories, as well as acoustic measurements. This model replaces the first generation blade rate model reported in ref. [16].

The major deficiencies in the modeling process are the scarcity of cavity observations which form the basis of the model, a



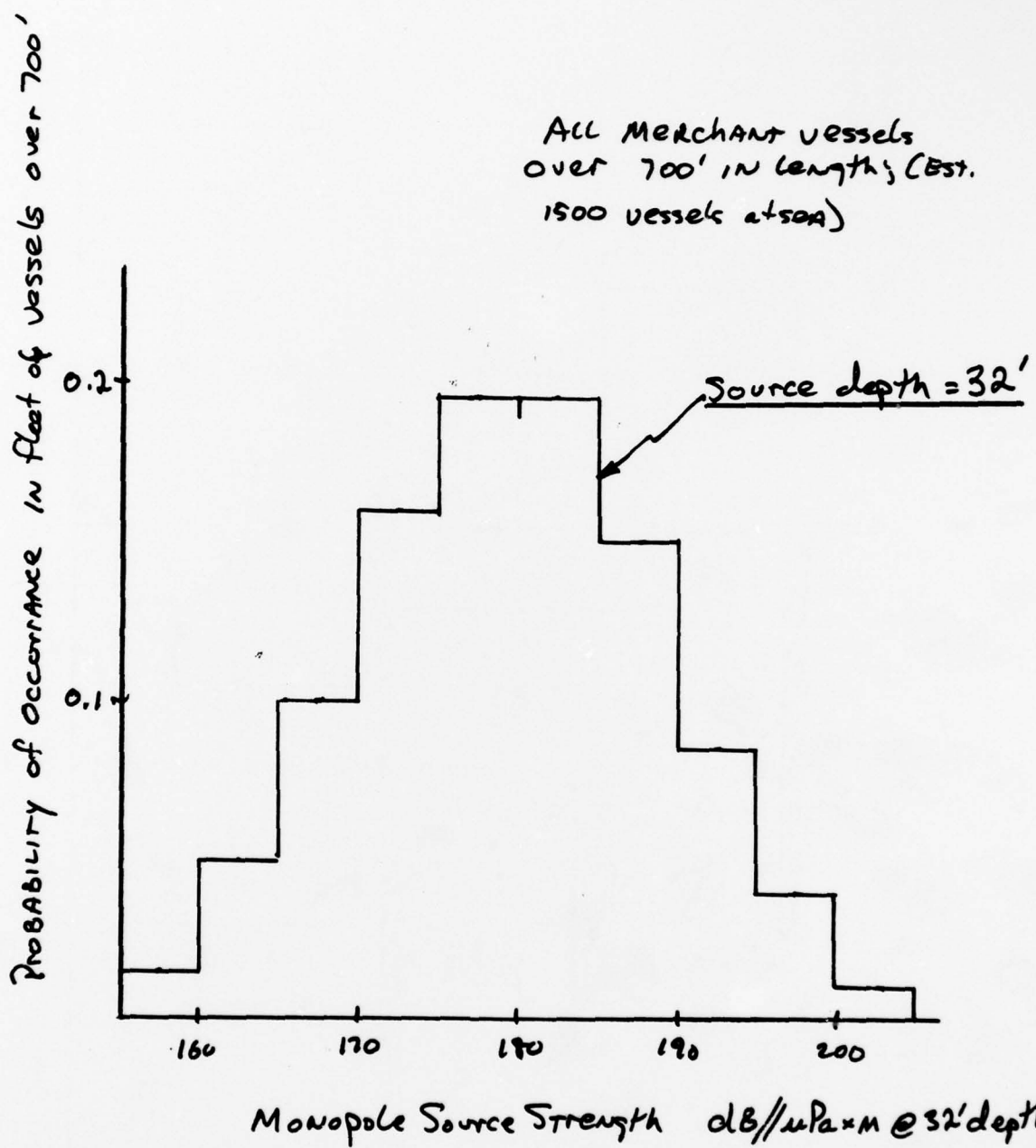


Figure 17: Monopole Source Strength PDF for BLADE
RATE OF THE MERCHANT fleet over 700' in length

lack of information on the higher harmonics of blade rate, and uncertainties in the modeling of acoustic radiation from this volume source.

Work is presently being conducted on modeling the acoustic radiation from this source and on limits imposed on the higher harmonics by volume dynamics. It is suggested that other sources of non-acoustic cavitation information be analyzed to refine the assumptions of figure 9. These sources should include proprietary measurements conducted by several of the European ship research facilities, which are not available in the open literature.

REFERENCES

- 1) Comstock, J.P. (ed.), "Principles of Naval Architecture", SNAME, New York, 1967.
- 2) Van Oossanen, P., "Calculation of Performance and Cavitation Characteristics of Propellers Including Effects of Non-Uniform Flow and Viscosity", NSMB Pub. 457, 1974.
- 3) Restad, K., Kjellberg, A., "Full Scale Measurements on Propeller Hull Interaction", Symposium on High Powered Propulsion of Large Ships, NSMB Pub. 490, 1974.
- 4) Holden, K., and Sontvedt, T., "On Stability and Volume of Marine Propeller Cavitation and Corresponding Spectral Distribution in Hull Pressure Fields", NSMB Pub. 490, 1974.
- 5) Sontvedt, T., Frivold, H., "Low Frequency Variation of the Surface Shape and Tip Region Cavitation on Marine Propeller Blades and Corresponding Disturbances on Nearly Solid Boundaries", Eleventh Symposium on Naval Hydrodynamics, London, April 1976.
- 6) Morgan, W., Cumming, R., "Propeller Design Aspects of Large, High Speed Ships", NSMB Pub. 490 1974.
- 7) Laredo, A., Beghin, D., Garguet, M., "Design of the First Generation of 550,000 DWT Tankers", Trans. SNAME, 1977.
- 8) Cremer, Heckl, Ungar, E., "Structureborne Sound", Springer-Verbag, New York, 1973.
- 9) Reed, E.F., "Acceptable Levels of Vibration on Ships", Marine Technology, April 1973.
- 10) Vossnack, E., Voogd, A., "Developments of Ship Afterbodies, Propeller Excited Vibrations", Second Lips Propeller Symposium, May 1973.

- 11) Greeley, D., "Calculation of Low Frequency Cavitation Source Strength of Marine Propellers", BBN Technical Memorandum No. 459, July 1978.
- 12) Shooter, J., Peterman, K.R., "Merchant Ship Signatures", ARL Report ARL-TR-77-47; August, 1977.
- 13) Cybulski, J., "Probable Origins of Measured Supertanker Radiated Noise Spectra", OCEANS '77 Conference Record, Vol. 1 October 1977.
- 14) Noordzij, L., "Pressure Field Induced by a Cavitating Propeller", International Shipbuilding Progress, Vol. 23, April 1976.
- 15) Lloyds, Inc., "Lloyds Register of Shipping Statistical Tables, 1972", Lloyds, London, 1972.
- 16) Hiene, J., Gray, L., "Merchant Ship Radiated Noise Model", BBN Report No. 3020, August 1976.